

# Mn 3d partial density of states in $\text{Ga}_{1-x}\text{Mn}_x\text{As}$ studied by resonant photoemission spectroscopy

J. Okabayashi

*Department of Physics, University of Tokyo, Bunkyo-ku, Tokyo 113-0033, Japan*

A. Kimura

*Synchrotron Radiation Laboratory, Institute for Solid State Physics, University of Tokyo, Roppongi, Minato-ku, Tokyo 106-8666, Japan*

T. Mizokawa and A. Fujimori

*Department of Physics, University of Tokyo, Bunkyo-ku, Tokyo 113-0033, Japan*

T. Hayashi and M. Tanaka

*Department of Electronic Engineering, University of Tokyo, Bunkyo-ku, Tokyo 113-0033, Japan*

(Received 7 July 1998; revised manuscript received 30 October 1998)

We have obtained the Mn 3d partial density of states in  $\text{Ga}_{1-x}\text{Mn}_x\text{As}$  using the resonance photoemission technique as well as by means of the difference between  $\text{Ga}_{1-x}\text{Mn}_x\text{As}$  and GaAs. We have observed a strong satellite structure on the higher binding energy side of the main peak, as in Mn-doped II-VI compounds such as  $\text{Cd}_{1-x}\text{Mn}_x\text{Te}$ . Based on analysis using configuration-interaction calculation for a  $\text{MnAs}_4$  cluster, we could ascribe the spectral features to strong Mn 3d-As 4p hybridization and Mn 3d-3d Coulomb interaction.

[S0163-1829(99)50904-1]

In the field of semiconductor physics, band theory based on the one-electron approximation has been very successful, and the electronic structure of impurities has been described using the effective mass theory for shallow levels, or using the Green function method for deep levels.<sup>1</sup> For transition-metal impurities in semiconductors it has become clear in recent years that it is essential to treat electron correlation effects explicitly. That is, one must treat hybridization between the localized electrons of the magnetic impurities and the delocalized band electrons of the host semiconductor. Transition-metal impurities in II-VI semiconductors have been extensively studied because the host can accommodate a high concentration of Mn and some other transition-metal ions. Diluted magnetic semiconductors (DMS) of Mn-doped II-VI compounds are now utilized in magneto-optical devices.<sup>2</sup> The recent development of synthesizing III-V based DMS such as  $\text{Ga}_{1-x}\text{Mn}_x\text{As}$  by molecular beam epitaxy has opened up new opportunities in the field of DMS.<sup>3</sup> The III-V based DMS show such remarkable properties as carrier-induced ferromagnetism and associated magnetotransport properties. A current issue is the microscopic origin of the carrier-induced ferromagnetism in the Mn-doped III-V based DMS. It is known that the transition-metal impurities in the II-VI based DMS behave as 2+ cations.<sup>4</sup> On the other hand, it has been controversial which valence state of the Mn impurity is stable in the III-V based DMS.

In order to elucidate the magnetic and transport properties of the III-V based DMS, it is necessary to obtain information about their valence-band electronic structure, including the  $p$ - $d$  exchange interaction between the Mn 3d electrons and the band electrons. In previous work,<sup>5</sup> we have made core-level x-ray photoemission spectroscopy (XPS) measurements of  $\text{Ga}_{1-x}\text{Mn}_x\text{As}$  and estimated the  $p$ - $d$  hybridization strength and the occupation number of the Mn 3d orbitals using configuration-interaction (CI) cluster model analysis.<sup>6</sup>

Photoemission spectroscopy in the valence-band region has also been extensively used to study the electronic structure of strongly correlated electron systems such as high-temperature superconductors and Mott insulators.<sup>7</sup> In the studies of the II-VI based DMS, too, photoemission spectroscopy has been a powerful technique to investigate their valence-band electronic structure.<sup>8,9</sup> In this work, valence-band photoemission studies have been performed and the Mn 3d density of states (DOS) in  $\text{Ga}_{1-x}\text{Mn}_x\text{As}$  has been deduced.

The photoemission experiments were performed at BL-18A of the Photon Factory, High Energy Accelerator Research Organization. Resonant photoemission experiments were made in an ultrahigh vacuum of  $10^{-11}$  Torr at room temperature. Photoelectrons were collected using a VG CLAM hemispherical analyzer in the angle-integrated mode. The resolution was estimated to be 100–200 meV from the Fermi edge of Ta foils.  $\text{Ga}_{1-x}\text{Mn}_x\text{As}$  (001) thin films with  $x=0.069$  and 0.035 were grown on GaAs (001) substrates by molecular beam epitaxy at a low growth temperature of 250 °C.<sup>10</sup> The Curie temperature was estimated from anomalous Hall effect to be 45–50 K.<sup>11</sup> For sample surface cleaning, we made Ar-ion sputtering at 1 kV and annealing up to 240 °C. The cleaned surfaces were checked by low-energy electron diffraction (LEED) and XPS measurements. We repeated Ar-ion sputtering and annealing until the O 1s and C 1s peaks in XPS were diminished below the detectability limit. Clear LEED patterns reflected ordered clean surfaces. After sputtering and annealing, the Mn content may change from the bulk value but the Mn core-level XPS intensity agreed to within  $\pm 20\%$  with the bulk values, which have been determined from the electron probe microanalysis.<sup>10</sup>

The Mn 3p-to-3d core absorption occurs at photon energies above 50 eV. Interference between the normal photoemission and the Mn 3p-to-3d transition followed by a

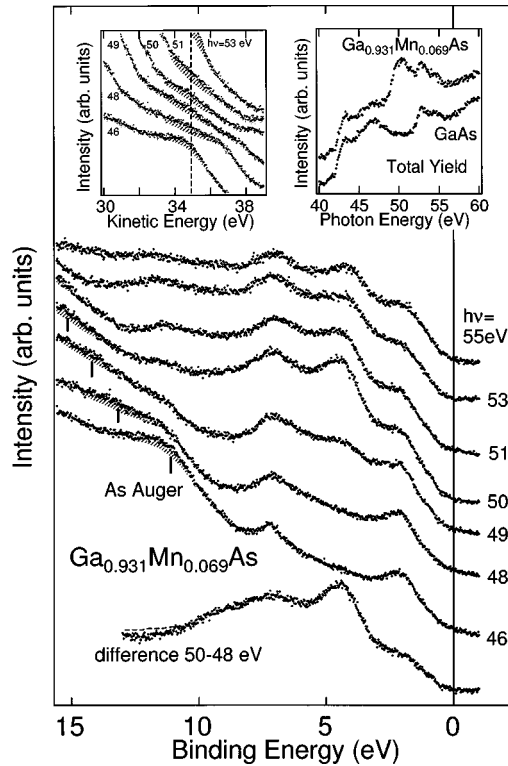


FIG. 1. A series of photoemission spectra of  $\text{Ga}_{1-x}\text{Mn}_x\text{As}$  for various photon energies near the Mn  $3p \rightarrow 3d$  core excitation threshold. The hatched area is the As Auger contribution estimated as shown in the left inset. The vertical bars denote the constant kinetic energy. The difference between the on-resonant ( $h\nu = 50$  eV) and off-resonant (48 eV) spectra, which is a measure of the Mn  $3d$  partial density of states, is shown at the bottom. Here, the dashed curve is the spectrum obtained by correcting for the As Auger emission. The right inset shows the absorption spectra of  $\text{Ga}_{0.931}\text{Mn}_{0.069}\text{As}$  and GaAs recorded by the total electron yield method.

$3p$ - $3d$ - $3d$  Coster-Krönig decay generates a resonance in the valence-band spectra. From such measurements, we could obtain a resonantly enhanced Mn  $3d$  partial DOS in the valence-band spectra. The right inset of Fig. 1 shows the absorption spectra of  $\text{Ga}_{0.931}\text{Mn}_{0.069}\text{As}$  and GaAs recorded in the total electron yield method. They indeed show a strong absorption peak at 50 eV originated from Mn. The peak at 42 eV is the As  $3d$  core absorption. From the absorption spectrum, the resonant and off-resonant photon energies are found to be 50 eV and 48 eV, respectively.

The valence-band spectra taken at various photon energies are shown in Fig. 1. Here, the intensities have been normalized to the photon flux. All the binding energies are referenced to the Fermi energy ( $E_F$ ). One can see that in going from  $h\nu = 46$  to 50 eV, the peak at a binding energy ( $E_B$ ) of 4.5 eV grows in intensity. One can also see a broad feature from  $E_B = 6$  to 10 eV, whose intensity grows in going from  $h\nu = 46$  to 50 eV. This broad feature is therefore attributed to the Mn  $3d$  origin. It should be noticed that Auger emission from the As  $3d$  core level overlaps and moves to higher binding energies as the photon energy increases as shown by a hatched area in Fig. 1. In order to subtract out the As Auger contribution, we exploited the fact that the Auger features have the same kinetic energies and the same area

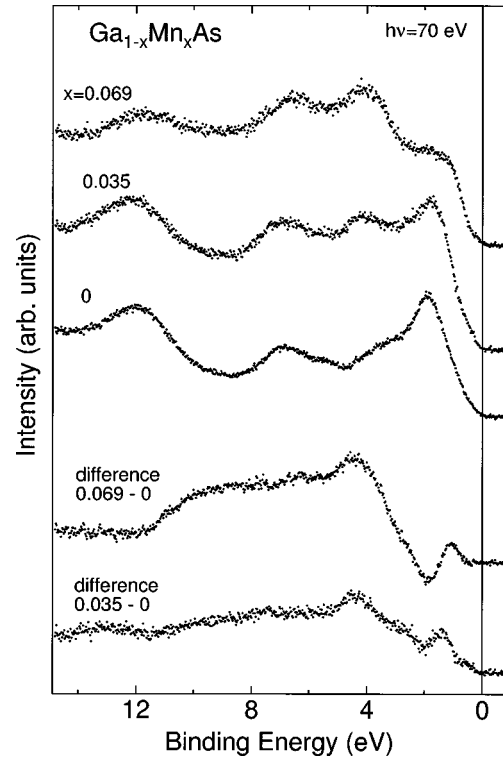


FIG. 2. Photoemission spectra of  $\text{Ga}_{1-x}\text{Mn}_x\text{As}$  ( $x = 0.035, 0.069$ ) and the GaAs substrate ( $x = 0.0$ ) for  $h\nu = 70$  eV, where the Mn  $3d$  cross section is large compared to As  $4p$ .

was assumed for the spectrum of each energy as shown in the left inset of Fig. 1.

By subtracting the off-resonant ( $h\nu = 48$  eV) spectrum from the on-resonant (50 eV) one, we obtained the Mn  $3d$  partial DOS as shown in the bottom panel of Fig. 2. Here, based on the As  $4p$  cross section for  $h\nu = 50$  and 48 eV, which are estimated to be 0.17 and 0.3 (in arbitrary units), respectively,<sup>12</sup> the 48 eV spectrum had been reduced prior to the subtraction in order to subtract out the As  $4p$  contribution. The difference spectrum thus obtained that corresponds to the Mn  $3d$  partial DOS indicates the main peak at 4.5 eV and a strong satellite at 6–10 eV. The spectrum also shows a broad feature at a lower binding energy of  $\sim 2$  eV. The satellite at  $E_B = 6$ –10 eV cannot be reproduced by the band-structure calculation for a hypothetical zinc-blende type MnAs and  $\text{Ga}_{0.5}\text{Mn}_{0.5}\text{As}$  (supercell) (Ref. 13) and would therefore be attributed to a many-electron effect. The line shape of the Mn  $3d$  partial DOS is thus similar to that of the Mn-doped II-VI compounds.<sup>14,8,9</sup> The position of the main peak ( $E_B = 4.5$  eV) in the present case may appear deeper than those in the II-VI based DMS ( $E_B = 3.5$  eV),<sup>8,9</sup> but this is largely due to the different energy references between the different studies: Binding energies were referenced to the top of the valence band in the studies of the II-VI compounds while they are referenced to  $E_F$  in the present study.

The difference spectra between  $\text{Ga}_{1-x}\text{Mn}_x\text{As}$  and pure GaAs were also used to obtain the Mn  $3d$  partial DOS as shown in Fig. 2. Here, the photon energy was fixed at  $h\nu = 70$  eV in order to increase the relative cross sections of Mn  $3d$  to As  $4p$ .<sup>12</sup> The intensities have been normalized to the Ga  $3d$  and As  $3d$  core-level spectra. The difference spectra thus obtained agree well with those obtained from the reso-

nant photoemission experiment except for the  $\sim 2$  eV feature. The structure around  $E_B \sim 2$  eV in the difference spectrum means that upon Mn doping the peak at  $E_B \sim 2$  eV in GaAs is weakened and a new structure appears at  $E_B \sim 1.5$  eV. This may be caused by a strong hybridization between the Mn 3d states and energy bands of GaAs around the van Hove singularity at the  $L$  point ( $L_3$  state),<sup>15</sup> causing the energy shift as large as  $\sim 0.5$  eV. That is, the binding energies of the  $p$ - $d$  hybridized states are shifted toward lower binding energy compared to the unhybridized states around the  $L_3$  state of GaAs. Recently magnetic circular dichroism (MCD) in the visible to ultraviolet region has been measured for  $\text{Ga}_{1-x}\text{Mn}_x\text{As}$  including the interband transition involving states around the  $L_3$  state,<sup>16</sup> consistent with the present study. The MCD result has revealed antiferromagnetic coupling between the Mn 3d and ligand As 4p orbitals in the strongly hybridized state.

The interpretation of the Mn 3d partial DOS that we have obtained has to be made beyond the one-electron approximation especially for the satellite structure. Ley *et al.*<sup>8</sup> made an analysis of the photoemission spectra of the II-VI based DMS,  $\text{Cd}_{1-x}\text{Mn}_x\text{Te}$ , using the CI cluster model. The calculation treats several electronic configurations with different  $d$ -electron numbers both in the initial and final states of photoemission. We considered the  $\text{MnAs}_4$  cluster as a model to analyze the Mn 3d partial DOS. Following the CI approach,<sup>8,17</sup> short-range interactions within the cluster are treated exactly. Although the cluster size may be small compared to the spatial extent to which the Mn impurity affects the electronic structure, the adjustable parameters of the model are considered as effective parameters that may also include longer-range interactions. Because of such characteristics, the CI cluster model well describes the Mn 3d partial DOS and is suited for the impurity systems. As for the parameters of the CI cluster model, the charge-transfer energy from the ligand As 4p orbitals to the Mn 3d orbitals is defined by  $\Delta$ , the 3d-3d Coulomb interaction by  $U$ , and the hybridization between the Mn 3d and As 4p orbitals by Slater-Koster parameters by  $(pd\sigma)$  and  $(pd\pi)$ . A hole in the ligand As 4p orbitals is denoted by  $\underline{L}$ . The ligand-to-Mn 3d charge-transfer state is written as  $d^5\underline{L}$  and two-electron-transferred state as  $d^6\underline{L}^2$ . We used Racah parameters to incorporate multiplet effects.<sup>18</sup> The relation  $(pd\sigma)/(pd\pi) = -2.17$  was assumed.<sup>19</sup> The Mn 3d partial DOS was fitted using nearly the same parameters as those used for the fitting of the Mn 2p core-level spectra. We have assumed the wave function of the ground state as a linear combination of  $d^5, d^6\underline{L}, d^7\underline{L}^2, \dots$ , configurations. Namely, we have assumed that the valence state of Mn is 2+ and the additional hole goes into the top of the valence band of GaAs. The best fit result is shown in Fig. 3 with parameter values  $\Delta = 1.5 \pm 1$  eV,  $U = 3.5 \pm 1$  eV and  $(pd\sigma) = 1.0 \pm 0.1$  eV. This charge-transfer energy is generally smaller than that of II-VI based DMS; where  $\Delta$ ,  $U$ , and  $(pd\sigma)$  are 2.0, 4.0, and 1.1 for  $\text{Cd}_{1-x}\text{Mn}_x\text{Te}$ ; 3.0, 4.0, and 1.2 for  $\text{Cd}_{1-x}\text{Mn}_x\text{Se}$ ; and 4.0, 4.0, and 1.3 for  $\text{Cd}_{1-x}\text{Mn}_x\text{S}$ .<sup>14</sup> From the coefficients of the  $d^5, d^6\underline{L}, d^7\underline{L}^2, \dots$ , configurations for the ground-state wave function, the Mn 3d counts were found to be  $5.3 \pm 0.1$ . As shown in Fig. 3, the main peak largely consists of  $d^5\underline{L}$  final states and the satellite consists of  $d^4$  final states because

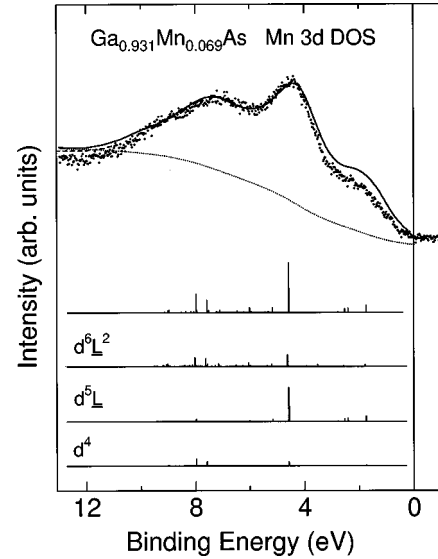


FIG. 3. Cluster-model analysis of the Mn 3d partial density of states assuming the  $\text{Mn}^{2+}$  valence state. The calculated spectrum is shown by a solid curve. The vertical bars are unbroadened spectra. In the bottom panel, the calculated spectrum is decomposed into  $d^4$ ,  $d^5\underline{L}$ , and  $d^6\underline{L}^2$  final-state components. The background is shown by a dotted curve. The dashed curve has been obtained by correcting for the overlapping As Auger emission (see Fig. 1).

$\Delta < U$ . Because of the small value of  $\Delta$ , not only  $d^4$  and  $d^5\underline{L}$  but also  $d^6\underline{L}^2$  states are important in the final state for constructing the Mn 3d spectra.

Within the one-electron picture, the Mn 3d level is exchange split into the spin-up and spin-down states, each of which is further split into the  $t_2$  and  $e$  sublevels through hybridization with the tetrahedrally coordinated ligand As 4p orbitals. From symmetry, the Mn 3d- $t_2$  orbitals hybridize more strongly with the ligand As 4p orbitals. The Mn 3d- $e$  orbitals are relatively well localized and more strongly contribute to the main peak of the Mn 3d DOS. The electronic structure of  $\text{Ga}_{1-x}\text{Mn}_x\text{As}$ , however, has to be treated as a many-electron system. In the CI cluster model analysis, we have assumed that the Mn ion is the  $\text{Mn}^{2+}$  valence state. For the  $\text{Mn}^{2+}$  state, the  $p$ - $d$  exchange interaction should be antiferromagnetic, consistent with the MCD result.<sup>14,16</sup> If we assumed the  $\text{Mn}^{3+}$  valence state,  $\Delta$  would be negative and the calculated spectrum would be similar to that of  $\text{Mn}^{2+}$ , as found in the previous core-level study.<sup>5</sup> Although the MCD result is in favor of the  $\text{Mn}^{2+}$  state and the photoemission results are consistent with  $\text{Mn}^{2+}$ , we need further experimental confirmation of the Mn valence state by, e.g., core-level MCD experiment.<sup>20</sup> In the present spectra, the DOS at  $E_F$  is small and no clear Fermi edge is observed in spite of the metallic conductivity in the  $x=0.035$  sample, although the band-structure calculation for  $\text{Ga}_{1-x}\text{Mn}_x\text{As}$  has shown a clear Fermi edge.<sup>13</sup> This may be attributed to the low carrier concentration and the poor metallic conductivity in  $\text{Ga}_{1-x}\text{Mn}_x\text{As}$ . In order to understand the low DOS at  $E_F$ , electron correlation and disorder would also have to be taken into account. Whether the doped holes in  $\text{Ga}_{1-x}\text{Mn}_x\text{As}$  has Mn 3d character or not is not obvious but the high Mn 3d partial DOS near the top of the valence band found in the present study suggests that a significant amount of Mn 3d

character is mixed in the doped holes.

In conclusion, the resonant photoemission and subsequent cluster-model analysis have revealed strong hybridization between the Mn 3d orbitals and the band electrons of the host semiconductor GaAs as well as the strong Mn 3d-3d on-site Coulomb interaction. The Mn 3d DOS between  $E_B \sim 6$  and 10 eV is a satellite, which is found to be unscreened Mn 3d<sup>4</sup> final states according to the cluster-model analysis. The charge-transfer energy from the ligand As 4p orbitals to the Mn 3d ones is found to be small compared with the II-VI compounds. While the valence of the Mn ion has been as-

sumed to be Mn<sup>2+</sup>, and the Mn 3d counts is found to be as large as  $5.3 \pm 0.1$ .

The authors would like to thank M. Shirai for valuable discussions, O. Rader and A. Kakizaki for useful advice and continuous support, and A. Harasawa, K. Kobayashi, A. Ino, T. Yoshida, and M. Satake for technical support. This work was supported by a Grant-in-Aid for Scientific Research on the Priority Area "Spin Controlled Semiconductor Nanostructures" from the Ministry of Education, Science, Sports and Culture. This work was performed under the approval of the Photon Factory Program Advisory Committee (Contract No. 97G335).

- 
- <sup>1</sup>M. Lanoo and J. Bourgoin, *Point Defects in Semiconductors* (Springer-Verlag, Berlin, 1981).
- <sup>2</sup>K. Onodera, T. Matsumoto, and M. Kimura, *Electron. Lett.* **30**, 1954 (1994).
- <sup>3</sup>H. Ohno, H. Munekata, T. Penny, S. von Molnar, and L. L. Chang, *Phys. Rev. Lett.* **68**, 2664 (1992).
- <sup>4</sup>J. K. Furdyna, *J. Appl. Phys.* **64**, R29 (1988); S. H. Wei and A. Zunger, *Phys. Rev. B* **35**, 2340 (1987).
- <sup>5</sup>J. Okabayashi, A. Kimura, O. Rader, T. Mizokawa, A. Fujimori, T. Hayashi, and M. Tanaka, *Phys. Rev. B* **58**, 4211 (1998).
- <sup>6</sup>A. E. Bocquet, T. Saitoh, T. Mizokawa, and A. Fujimori, *Solid State Commun.* **83**, 11 (1992).
- <sup>7</sup>M. Imada, A. Fujimori, and Y. Tokura, *Rev. Mod. Phys.* **70**, 1039 (1998).
- <sup>8</sup>L. Ley, M. Taniguchi, J. Ghijsen, R. L. Johnson, and A. Fujimori, *Phys. Rev. B* **35**, 2839 (1987).
- <sup>9</sup>M. Taniguchi, A. Fujimori, M. Fujisawa, T. Mori, I. Souma, and Y. Oka, *Solid State Commun.* **62**, 431 (1987).
- <sup>10</sup>T. Hayashi, M. Tanaka, T. Nishinaga, H. Shimada, H. Tsuchiya, and Y. Otuka, *J. Cryst. Growth* **175/176**, 1063 (1997).
- <sup>11</sup>T. Hayashi, M. Tanaka, T. Nishinaga, and H. Shimada, *J. Appl. Phys.* **81**, 4865 (1997).
- <sup>12</sup>J. J. Yeh and I. Lindau, *At. Data Nucl. Data Tables* **32**, 1 (1985).
- <sup>13</sup>M. Shirai, T. Ogawa, I. Kitagawa, and N. Suzuki, *J. Magn. Magn. Mater.* **177-181**, 1383 (1998).
- <sup>14</sup>T. Mizokawa and A. Fujimori, *Phys. Rev. B* **48**, 14 150 (1993).
- <sup>15</sup>L. Ley, R. A. Pollak, F. R. McFeely, S. P. Kowalszyk, and D. A. Shirley, *Phys. Rev. B* **9**, 600 (1974).
- <sup>16</sup>K. Ando, T. Hayashi, M. Tanaka, and A. Twardowski, *J. Appl. Phys.* **53**, 6548 (1998).
- <sup>17</sup>A. Fujimori and F. Minami, *Phys. Rev. B* **30**, 957 (1984).
- <sup>18</sup>S. Sugano, Y. Tanabe, and H. Kaminura, *Multiplets of Transition Metal Ions in Crystals* (Academic Press, New York, 1970).
- <sup>19</sup>W. A. Harrison, *Electronic Structure and the Properties of Solids* (Dover, New York, 1989).
- <sup>20</sup>A. Kimura, S. Suga, T. Shishidou, S. Imada, T. Muro, S. Y. Park, T. Miyahara, T. Kaneko, and T. Kanomata, *Phys. Rev. B* **56**, 6021 (1997).